Psychiatry Research: Neuroimaging 333 (2023) 111660

Contents lists available at ScienceDirect

Psychiatry Research: Neuroimaging

journal homepage: www.elsevier.com/locate/psychresns

Striatal dopamine in anhedonia: A simultaneous [^{11}C]raclopride positron emission tomography and functional magnetic resonance imaging investigation

Rachel D. Phillips [a,*], Erin C. Walsh [b], Nicole R. Zürcher [g], David S. Lalush [c], Jessica L. Kinard [d], Chieh-En Tseng [g], Paul M. Cernasov [a], Delia Kan [d], Kaitlin Cummings [a], Lisalynn Kelley [e], David Campbell [e], Daniel G. Dillon [f], Diego A. Pizzagalli [f], David Izquierdo-Garcia [g], Jacob M. Hooker [g], Moria J. Smoski [e], Gabriel S. Dichter [a,b,d]

[a] Department of Psychology and Neuroscience, University of North Carolina-Chapel Hill, Chapel Hill, NC, United States
[b] Department of Psychiatry, University of North Carolina-Chapel Hill, Chapel Hill, NC, United States
[c] Joint Department of Biomedical Engineering, University of North Carolina at Chapel Hill and North Carolina State University, Raleigh, NC, United States
[d] Carolina Institute for Developmental Disabilities, University of North Carolina at Chapel Hill School of Medicine, Chapel Hill, Chapel Hill, NC, United States
[e] Department of Psychiatry & Behavioral Sciences, Duke University, Durham, NC, United States
[f] Center for Depression, Anxiety and Stress Research, McLean Hospital, Belmont, MA, United States
[g] Athinoula A. Martinos Center for Biomedical Imaging, Department of Radiology, Massachusetts General Hospital, Harvard Medical School, Charlestown, MA, United States

ARTICLE INFO

Keywords:
Anhedonia
Dopamine
PET-MR
Reward
Mesolimbic
Self-reported stress

ABSTRACT

Background: Anhedonia is hypothesized to be associated with blunted mesocorticolimbic dopamine (DA) functioning in samples with major depressive disorder. The purpose of this study was to examine linkages between striatal DA, reward circuitry functioning, anhedonia, and, in an exploratory fashion, self-reported stress, in a transdiagnostic anhedonic sample.

Methods: Participants with (n = 25) and without (n = 12) clinically impairing anhedonia completed a reward-processing task during simultaneous positron emission tomography and magnetic resonance (PET-MR) imaging with [^{11}C]raclopride, a DA D2/D3 receptor antagonist that selectively binds to striatal DA receptors.

Results: Relative to controls, the anhedonia group exhibited decreased task-related DA release in the left putamen, caudate, and nucleus accumbens and right putamen and pallidum. There were no group differences in task-related brain activation (fMRI) during reward processing after correcting for multiple comparisons. General functional connectivity (GFC) findings revealed blunted fMRI connectivity between PET-derived striatal seeds and target regions in the anhedonia group. Associations were identified between anhedonia severity and the magnitude of task-related DA release to rewards in the left putamen, but not mesocorticolimbic GFC.

Conclusions: Results provide evidence for reduced striatal DA functioning during reward processing and blunted mesocorticolimbic network functional connectivity in a transdiagnostic sample with clinically significant anhedonia.

1. Introduction

Anhedonia is characterized by impaired reward processing and blunted mesocorticolimbic dopamine (DA) system functioning (Borsini et al., 2020; Berridge and Kringelbach, 2008; Pizzagalli, 2014). This ascending DA tract passes through reward learning (-*meso*), cognitive control (-cortico), and emotional (-limbic) hubs of the brain (Berridge and Robinson, 2003), and impairments in motivation and the anticipation of rewards are associated with alterations in striatal DA tone, DA release, and DA signaling (Pizzagalli, 2014; Russo and Nestler, 2013; Schultz, 2019; Der-Avakian and Markou, 2012). Associations between anhedonia and mesocorticolimbic DA system functioning have primarily been investigated in major depressive disorder (MDD) (Peciña et al., 2017; Pizzagalli et al., 2019). While anhedonia is a core symptom of

* Corresponding author
E-mail address: Rachel.phillips@unc.edu (R.D. Phillips).

https://doi.org/10.1016/j.pscychresns.2023.111660
Received 7 November 2022; Received in revised form 21 April 2023; Accepted 18 May 2023
Available online 1 June 2023

MDD, it is also a transdiagnostic symptom that is pervasive across numerous neuropsychiatric disorders (Husain and Roiser, 2018). A putative neural mechanism of anhedonia is striatal hypoactivation, and anhedonia severity negatively correlates with ventral striatal activity during the anticipation of rewards in depressed populations (Stringaris et al., 2015; Stringaris et al., 2015; Arrondo et al., 2015). Anhedonia severity is also associated with altered intrinsic functional connectivity between striatal regions and areas of the prefrontal cortex (PFC) in adolescents (Gabbay et al., 2013) and adults (Liu et al., 2021; Felger et al., 2015). In a non-clinical adult sample, reduced nucleus accumbens response to reward was uniquely related to anhedonia severity, and not depressive or anxious symptoms (Wacker et al., 2009). Together these findings demonstrate distinct patterns of mesocorticolimbic DA system activation and connectivity associated with anhedonia.

Simultaneous positron emission tomography and magnetic resonance (PET-MR) imaging using [^{11}C]raclopride, a radioligand that allows for the quantification of DA D2/D3 receptor binding, has demonstrated that functional magnetic resonance imaging (fMRI) activation and functional connectivity in mesolimbic brain regions during reward anticipation correlate with ventral striatal DA release in MDD (Hamilton et al., 2018) and non-clinical (Schott et al., 2008) samples. Anhedonia is associated with altered DA functioning, including decreased striatal DA transporter availability in MDD (Pizzagalli et al., 2019) and increased striatal DA D2/D3 receptor availability in MDD (Peciña et al., 2017), although no association between anhedonia and DA release capacity in MDD has been reported (Schneier et al., 2018). This inconsistency may be explained, in part, by the diagnostic heterogeneity of MDD as opposed to sampling an anhedonic phenotype.

Additionally, alterations in DA signaling, and mesocorticolimbic DA system functioning more broadly, are linked to stress (Pizzagalli, 2014; Der-Avakian and Markou, 2012; Stanton et al., 2018; Kumar et al., 2015). Considerable animal research on this topic supports the idea that chronic, uncontrollable, and unpredictable stressors impact DA signaling (Cabib and Puglisi-Allegra, 2012) thereby contributing to the emergence of anhedonic-like behaviors, such as reduced sucrose preference or intake (Antoniuk et al., 2019) and learned helplessness (Willner et al., 1992; Riga et al., 2015; Krishnan et al., 2007). Within human samples, stress is also associated with neural and behavioral deficits in reward processing, including reduced goal-directed behavior, blunted incentive motivation, impaired reward learning, and alterations in striatal activation and connectivity during anticipation and receipt of rewards (Pizzagalli, 2014; Hollon et al., 2015; Soares et al., 2012; Hanson et al., 2021). However, no research has examined associations between self-reported stress, anhedonia, and striatal dopamine functioning in a transdiagnostic anhedonic sample.

In the present study, we used simultaneous PET-MR imaging with the D2/D3 dopamine receptor antagonist [^{11}C]raclopride in a transdiagnostic sample of adults with clinically impairing anhedonia to investigate relationships between anhedonia, striatal DA release, and mesocorticolimbic network functioning during reward processing. We hypothesized that the transdiagnostic anhedonia group would be characterized by decreased striatal task-related DA release to rewards, indexed by the non-displaceable binding potential (ΔBP_{ND}) of [^{11}C]raclopride, relative to a control group. We also hypothesized that striatal DA functioning would predict anhedonia severity. Next, we predicted that the anhedonia group would show decreased mesocorticolimbic network activation and connectivity during reward processing using fMRI. Finally, an exploratory aim was to examine associations between self-reported stress, anhedonia, and mesocorticolimbic DA system functioning. This aim was exploratory given that participants were not recruited based on stress exposure. We hypothesized that greater self-reported stress would be inversely associated with striatal DA release and mesocorticolimbic network fMRI activation and connectivity during reward processing.

2. Methods

2.1. Study overview

The present study complements an ongoing NIMH-funded clinical trial (R61/R33 MH110027) investigating the effects of a novel psychosocial anhedonia treatment on neural responses to rewards and anhedonia symptoms (ClinicalTrials.gov Identifiers NCT02874534 and NCT04036136). Data from control participants, recruited as part of a separate study, have been reported previously (Zürcher et al., 2021). These companion studies met research standards for Institutional Review Board (IRB) approval at UNC—Chapel Hill and Duke University, and PET imaging protocols were approved by the UNC Radioactive Drug Research Committee. PET-MR imaging data acquisition occurred within four weeks of completing inclusion and exclusion assessment, and prior to randomization into psychotherapy treatment groups, for the companion study. Written informed consent was obtained prior to inclusion in the study.

2.2. Participants

2.2.1. Eligibility criteria

Eligible participants in the ANH group were 18 to 50 years old, treatment-seeking for clinically significant anhedonia (i.e., Snaith-Hamilton Pleasure Scale (SHAPS) scores greater than or equal to 20 using the ordinal scoring of Franken and colleagues (Franken et al., 2007) and with Clinician's Global Impression Scale Severity (CGI-S; (Kadouri et al., 2007) scores greater than or equal to 3, indicating clinical impairment). Eligible participants in the CON group had no present or past psychiatric diagnoses, as assessed by the Structured Clinical Interview for DSM-5 (SCID-5-RV) (First et al., 2015). Additional eligibility criteria are provided in Supplemental Materials IA.

Twenty-eight ANH participants and 23 CON participants completed PET-MR scans. Three ANH participants and 11 CON participants were excluded due to problems with the PET injection or scanner (4 CON participants), PET infusion (2 ANH participants), or technical errors at the scan (1 ANH and 7 CON participants). The final sample included 25 ANH participants and 12 CON participants.

2.3. Clinical diagnostic & symptom measures

The SCID-5-RV was used to assess eligibility and for clinical characterization. (Zürcher et al., 2021) Only participants in the ANH group completed the following self-report measures assessing stress and anhedonia severity.

The Perceived Stress Scale (PSS-10) was the primary measure of self-reported stress. The PSS assesses self-reported unpredictable and uncontrollable stressors over the past month and contains 10 items (Cohen et al., 1983). Total scores range from 0 to 40, whereby higher scores indicate greater perceived stress (Bernstein et al., 1994).

The posttraumatic stress disorder (PTSD) Checklist (PCL-5), the secondary measure of self-reported stress, was used to assess PTSD symptoms in the last month. The PCL-5 is a well-validated scale with 20 items (Blevins et al., 2015). Total scores range from 0 to 80, whereby higher scores indicate greater severity of symptoms. The PCL-5 version used in the current study did not include the Criterion A component. Therefore, scores reflect general distress in relation to stressful life events rather than a Criterion A trauma (Gasperi et al., 2021).

The Snaith–Hamilton Pleasure Scale (SHAPS) was the primary measure of anhedonia. The SHAPS is a well-validated 14-item questionnaire that assesses hedonic capacity. Total scores range from 14 to 56, whereby higher scores indicate greater anhedonia severity in the present state (i.e., "the last few days").

The 21-item Beck Depression Inventory (BDI-II) was administered to assess depression symptom severity. Total scores range from 0 to 63, whereby higher scores indicate greater depressive severity. The BDI-II

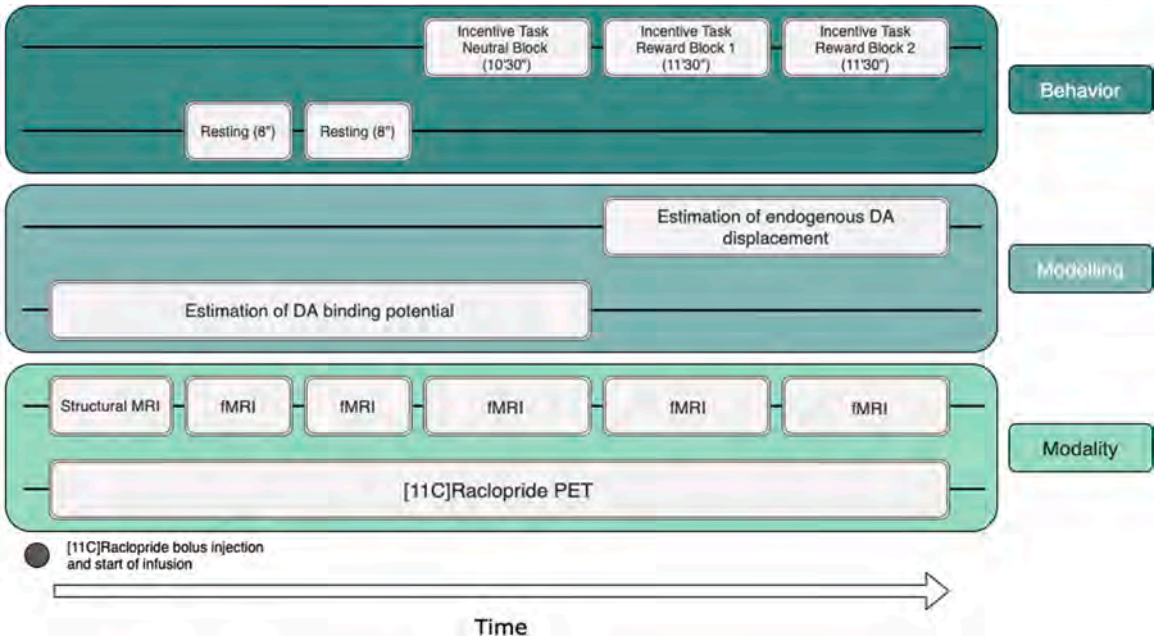

Fig. 1. Timing of data collection, data modeling, and participant behavior during scanning. Three task blocks were presented during which fMRI data were collected simultaneously with the PET acquisition.

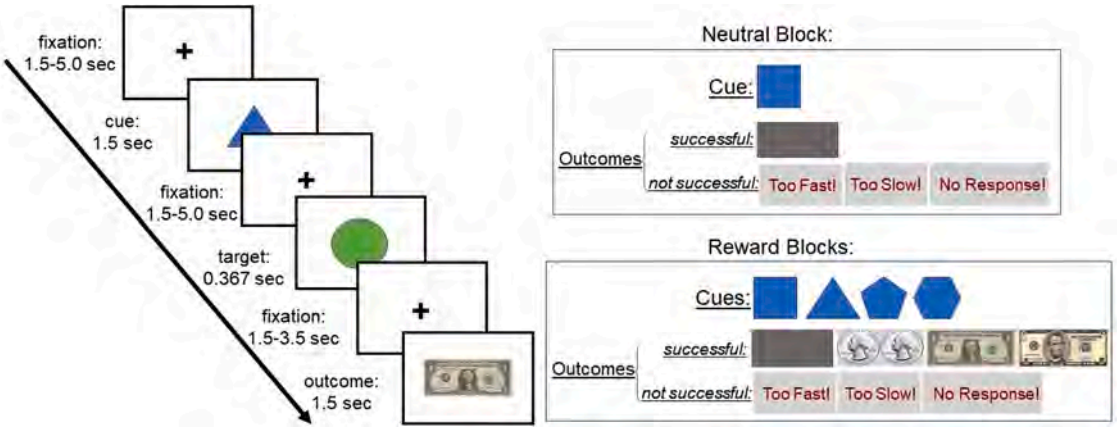

Fig. 2. PET-MR Monetary Incentive Delay (MID) Task.
Each trial consisted of a cue phase and an outcome phase. Trials were presented first in a neutral block that consisted of only neutral trials and then in two reward blocks that consisted of reward trials of varying magnitudes (small, medium, or large). The relationship between cue identity and outcome magnitude had to be learned by experience. Further details of the PET-MR Monetary Incentive Delay (MID) Task are provided in the Supplemental Materials IC.

Anhedonia Subscale was used as a secondary measure of anhedonia. This comprises four items from the BDI-II (i.e., loss of interest, loss of pleasure, loss of interest in sex, and loss of energy) (Pizzagalli et al., 2005). Whereas the SHAPS primarily assesses aspects of consummatory reward (Rizvi et al., 2016), the BDI-II anhedonia subscale captures aspects of both consummatory and anticipatory reward processing (Pizzagalli et al., 2005).

2.4. Neuroimaging data

2.4.1. Simultaneous pet-mr scan protocol and pre-processing

Participants completed a 75-minute simultaneous PET-MR scan on a Siemens Biograph mMR scanner using a bolus+infusion protocol (*Fig. 1*) with a planned K_{bol} of 105 min. List mode 3-D emission data were collected starting from bolus injection of [^{11}C]raclopride (~1 min after scan start time; administered using a Medrad® Spectris Solaris® EP MR Injection System) and continuing over the 75-minute scan. [^{11}C]Raclopride is a D2/D3 antagonist which selectively binds to striatal DA receptors (Papenberg et al., 2019). In the first portion of scan acquisition, participants completed two 8-minute resting-state scans and one 6-minute high resolution T1 scan (FOV = 256 mm, 111 mm resolution, TR = 2530 ms, TE = 1.69 ms, flip angle = 7°), to allow time for tracer uptake. In the second portion, participants completed a monetary incentive delay task (MID), developed at McLean Hospital (by DGD and DAP) and modified for use in PET-MR studies (Zürcher et al., 2021). Participants were provided instructions via an intercom (i.e., headphones) and informed when transitions took place between resting, structural, and functional fMRI sequences. Acquisition parameters were identical for the resting state and functional scans (echo planar imaging, FOV = 212 mm, 3.312 × 3.312 × 3.3 mm resolution, TR = 3000, TE = 30 ms, flip angle = 90°). The reward task used during scanning is described in Supplemental Materials IC and illustrated in *Fig. 2*.

Dynamic PET images were reconstructed from list mode data (reconstruction grid was 344 × 344 with 127 axial slices and a voxel size

of 2.086 mm × 2.086 mm × 2.032 mm) using the PseudoCT method (Ladefoged et al., 2017), which uses the subject's Dixon attenuation map and the T1 MPRAGE image to estimate a CT- equivalent attenuation map. Next, PET images underwent motion correction using the Realign procedure of SPM12. This method computes a rigid transformation for each time frame to align all to a common reference. As a quality-control measure, the motion-corrected frames were observed in cine mode to detect possible errors. In all but two cases, the motion correction was found to achieve good alignment (see Supplemental Materials IA). Structural MR images (T1 scans) were pre-processed using Freesurfer version 7.1.0. Functional MR images were pre-processed using FSL version 6.0. To control for excessive motion, we censored volumes that exceeded a framewise displacement threshold of 0.5 mm (Siegel et al., 2014). Lastly, functional connectivity data (i.e., resting-state and MID task runs) were preprocessed with the default preprocessing pipeline in the SPM12 CONN functional connectivity toolbox, version 19c (Whitfield-Gabrieli and Nieto-Castanon, 2012).

2.4.2. PET analysis

[^{11}C]Raclopride is a D2/D3 receptor antagonist, and therefore competes with endogenous DA for receptors. Binding potential (BP_{ND}), the ratio of selectively bound ligand to non-displaceable ligand in the tissue at equilibrium, was estimated from dynamic PET images for the baseline and reward phases of PET acquisition for each subject. It is worth noting that binding potential may relate to several factors including but not limited to 1) receptor density, 2) change in synaptic DA concentration resulting in increased occupancy (i.e., reduction in binding site availability), and 3) change in receptor state that influences raclopride Kd (e.g., conformational change, internalization, post-translational modification etc.). BP_{ND} was quantified using the simplified reference tissue model (SRTM) (Lammertsma and Hume, 1996). Thus, each time-activity curve was fit with an SRTM model with four parameters: Baseline BP_{ND}, Reward BP_{ND}, k_2, and R_1. The baseline phase was defined from start of acquisition to start of the reward phase, including both the uptake phase and the neutral task block. Cerebellum was used as the reference region. More details on the two-phase model are found in Supplemental Materials IB.

The two-phase SRTM model was applied to time-activity curves from regional data (striatal regions of the AAL3 atlas) as well as to individual voxels of the dynamic PET sequences to create voxel maps of baseline and reward BPND. For groupwise analysis, individual subject maps were transformed to common MNI space using mappings derived from SPM12 and each subject's T1 structural images.

Reward blocks encompass trials during which participants both anticipated and received rewards. Baseline BP_{ND} and change in BP_{ND} following reward task onset (Δ BP_{ND}%) measures DA functioning during the non-reward state (i.e., baseline) and activation (reward task-related) states, respectively. This approach measures the extent to which endogenous DA displaces the radiotracer. A typical DA response to rewards in the striatum would be indicated by lower BP_{ND} values during reward, relative to baseline, indicating that DA has increased and outcompeted the tracer for binding sites (Peciña et al., 2017). Accordingly, decreased ΔBP_{ND} is interpreted as increased task-related DA release.

To identify regions that showed between-group differences in ΔBP_{ND} from baseline to reward phases of the MID, for each subject, we estimated striatal DA functioning during uptake of the tracer and during each condition of the task. Here, we would expect negative ΔBP_{ND} values (Reward – Baseline) for controls if DA out-competes the tracer. A *z*-score statistical map representing the difference between groups and conditions (ANH - CON; Reward – Baseline) was created from subject images by contrasting voxel-wise ΔBP_{ND} (Reward – Baseline) maps. Thus, z-scores compare ΔBP_{ND} for the ANH group to ΔBP_{ND} for the CON group in such a way that positive z-scores indicate that anhedonic participants demonstrate less response in the expected direction than control participants (i.e., ΔBP_{ND} for the ANH group is less negative than ΔBP_{ND} for the CON group). This *z*-score statistical map was then thresholded at $z > 2.58$ (uncorrected) and anatomically constrained to the bilateral caudate nucleus, putamen, pallidum, and nucleus accumbens using masks from the Harvard-Oxford probabilistic atlas. We estimated group differences only in the striatum, given that [^{11}C]raclopride selectively binds to DA receptors in the striatum (Papenberg et al., 2019).

For each significant functionally-defined cluster that emerged from this contrast, condition-specific ΔBP_{ND} values were extracted per participant. To study the pattern of results in greater detail, these values were then compared by evaluating group (ANH, CON) × condition (reward, baseline) interactions via analyses of variance (ANOVAs). For a complete description of PET analyses see Supplemental Materials IB and (Sander et al., 2016).

2.4.3. fMRI activation analysis

To examine fMRI responses during reward anticipation, BOLD responses to reward cues of all magnitudes (small, medium, and large) vs. neutral cues were examined from cue onset to the end of the fixation period (i.e., the period between the cue and target onsets). To examine fMRI responses during reward processing, activation to successful vs. unsuccessful outcomes on reward trials of all magnitudes (small, medium, and large) were examined (i.e., the period between the start and end of feedback presentation; see Fig. 2). A priori hypothesis testing was conducted using a region of interest (ROI) approach. ROI analyses examined regions implicated in reward anticipation (i.e., bilateral nucleus accumbens, caudate, and putamen) and reward outcome (i.e., medial prefrontal cortex and anterior cingulate cortex). Using FSL featquery, we calculated mean BOLD percent signal change in these ROIs for each contrast of interest. Separate from ROI analyses, exploratory whole-brain voxel-wise analyses were also conducted. See Supplemental Materials IF for additional details about fMRI activation analyses.

2.4.4. fMRI connectivity analysis

A general functional connectivity (GFC) approach examined whole-brain connectivity using striatal PET-derived seed regions that displayed significant differences in ΔBP_{ND} for the contrast ANH - CON; Reward - Baseline of the MID task. GFC, a method that combines resting-state and task fMRI data, offers better test-retest reliability and higher estimates of heritability than intrinsic connectivity estimates from the same amount of resting-state data alone (Elliott et al., 2019). In the current study, the combination of two resting-state runs and three MID task blocks yielded approximately 45 min of fMRI data for connectivity analyses. This is critical given that >25 min of fMRI data are needed to reliably detect individual differences in connectivity (Anderson et al., 2011). Voxel-wise whole-brain connectivity was evaluated using the CONN Toolbox's seed-to-voxel analysis. Analyses corrected for multiple comparisons using a false-discovery rate (FDR) approach, at the familywise error (FWE) rate of $p < .05$.

2.5. Associations between PET-MR, anhedonia, and self-reported stress in the anhedonia group

To examine whether anhedonia severity and self-reported stress were associated with striatal DA function and mesocorticolimbic network functioning within the ANH group, we conducted statistical regression models in R, version 4.0.3 (Team RC 2020). Because only participants in the ANH group completed self-report measures assessing stress and anhedonia severity, analyses were limited to this group. PET-derived striatal ΔBP_{ND} and network functional connectivity values (i.e., fMRI-derived correlations between network regions with correlated BOLD signal change) were tested as individual predictors of anhedonia severity (i.e., SHAPS and BDI anhedonia subscale), in separate regressions. Additional regressions tested whether self-reported stress (i.e., PSS and PCL-5) predicted the magnitudes of these PET-

Table 1
Sample Characteristics.

Variable	Anhedonia Group ($n = 25$)			Control Group ($n = 12$)			Total Sample ($n = 37$)			Group Comparisons
	M	*SD*	*Range*	*M*	*SD*	*Range*	*M*	*SD*	*Range*	*Test Statistic, p-value*
Age (years)	26.32	6.01	19–42	25.67	4.30	21–36	26.40	5.49	19–42	$t(28.7) = -0.14$, p=.887
[^{11}C] raclopride dose (mCi)	13.27	1.28	9.88–15.74	11.73	2.13	8.10–15.01	12.77	1.74	8.10–15.74	$t(14.9) = 2.31$, p=.036
Variable	*Count*		*Percent*	*Count*		*Percent*	*Count*		*Percent*	*Test Statistic, p-value*
Sex										
Female	15		(60.0%)	2		(16.7%)	17		(45.9%)	$\chi^2(1) = 6.13$, $p = .013$
Male	10		(40.0%)	10		(83.3%)	20		(54.1%)	
Race										
White	13		(52.0%)	8		(66.7%)	21		(56.8%)	
Black / African American	3		(12.0%)	2		(16.7%)	5		(13.5%)	
Asian	7		(28.0%)	1		(8.3%)	8		(21.6%)	
American Indian / Alaska Native	1		(4.0%)	–		–	1		(2.7%)	
Other (Not Listed)	2		(8.0%)	–		–	2		(5.4%)	
Not Reported	–		–	1		(8.3%)	1		(2.7%)	
Ethnicity										
Hispanic	4		(16.0%)	2		(16.7%)	6		(16.2%)	
Non-Hispanic	21		(84.0%)	10		(83.3%)	31		(83.8%)	

Note – Participants were able to endorse one or more race categories.

Table 2
Anhedonia Group Clinical Characteristics.

Variable	Anhedonia Group ($n = 25$)		
	M	*SD*	*Range*
PSS	20.84	3.64	13 - 27
SHAPS	36.64	4.37	30 - 45
BDI-II Anhedonia Subscale	5.04	2.03	2 - 9
BDI-II Total	20.20	9.12	3 - 41
PCL-5	19.12	12.38	1 - 43
Primary Diagnosis (SCID-5-RV)			
No Current Diagnosis	6	(24%)	
Major Depressive Disorder (MDD)	9	(36%)	
Persistent Depressive Disorder (PDD)	3	(12%)	
Generalized Anxiety Disorder	3	(12%)	
Attention-Deficit Hyperactivity Disorder (ADHD)	2	(8%)	
Specific Phobia	1	(4%)	
Other Specified Anxiety Disorder	1	(4%)	

PSS – Perceived Stress Scale; SHAPS – Snaith-Hamilton Pleasure Scale; BDI-II – Beck Depression Inventory-II; PCL-5 – Posttraumatic Stress Disorder Checklist; SCID-5-RV – Structured Clinical Interview for DSM-5.

and fMRI-derived variables. Corrections for multiple comparisons were made within each set of hypotheses (i.e., correcting across regression analyses that examined whether striatal DA release to rewards, or ΔBP_{ND}, predicted anhedonia severity).

Lastly, bivariate Pearson correlations between clinical and PET-MR variables of interest were explored. Corrections for multiple comparisons were made within each set of analyses (i.e., clinical variables with striatal ΔBP_{ND} values and clinical variables with network functional connectivity values) using the false-discovery rate (FDR) method (Benjamani and Hochberg, 1995).

3. Results

3.1. Participant characteristics

Table 1 summarizes demographic information and descriptive statistics for the samples. *Table 2* reports clinical characteristics for the ANH group; the self-report measures assessing stress and anhedonia severity were not collected in the CON group.

ANH and CON groups did not differ in age ($t(28.7) = -0.14$, $p = .887$). There were significantly fewer females in the CON group ($\chi^2(1) = 6.13$, $p = .013$). [^{11}C]Raclopride dose differed between groups; for the ANH and CON groups, the average dose was 13.27 mCi ($SD = 1.28$) and 11.73 mCi ($SD = 2.14$), respectively ($t(14.9) = 2.31$, $p = .036$). Thus, analyses presented here controlled for sex and [^{11}C]Raclopride dose.

Table 3
Striatal Clusters demonstrating ANH - CON Group Differences in ΔBP_{ND} values (Reward - Baseline) at a threshold of $z > 2.58$ (uncorrected).

Cluster Label	Cluster Size	Max Z value	Max X	Max Y	Max Z	Group x Condition Interaction p-value
Left putamen	88	4.70	−22	4	12	.0006**
Right putamen/ pallidum	23	3.63	18	6	−4	.007**
Left caudate	23	3.33	−16	4	14	.010*
Left NAc and putamen	19	3.45	−12	6	−8	.009*

Contrast of ANH - CON; Reward - Baseline ΔBP_{ND} values. MNI Coordinates. For all clusters, the Group (ANH, CON) × Condition (Reward, Baseline) interaction effect on [^{11}C]raclopride ΔBP_{ND} values were significant, controlling for sex and [^{11}C]raclopride dose. This was expected given that ANOVA results are dependent on the cluster-defining contrast. p-values <0.05*, <0.01**, <0.001***. NAc, Nucleus Accumbens. ANH, Anhedonia participants. CON, Control participants.

ANH participants reported moderate levels of anhedonia, as assessed by the SHAPS, as well as moderate depressive symptoms, as assessed by the BDI-II (Smarr and Keefer, 2011). ANH participants' PSS scores reflect moderate stress (Cohen and Janicki-Deverts, 2012), and PCL-5 scores reflect mild stress (Blevins et al., 2015). Five ANH participants had PCL-5 scores of 33 or greater, indicating clinically significant PTSD symptoms.

Within the ANH group, males reported significantly greater perceived stress on the PSS than females ($t(22.7) = -2.73$, $p = .011$). Anhedonia severity ratings did not differ by sex. In the ANH group, scores on the SHAPS and BDI-II anhedonia subscale were positively correlated ($r = 0.65$, $p = .0005$) and PSS and BDI-II anhedonia subscale scores were positively correlated ($r = 0.47$, $p = .0179$). Six ANH participants did not meet criteria for any current diagnoses; however, each had a CGI-S score of 3, indicating clinical impairment. See Supplemental Materials IIA for task reaction time and valence ratings analyses.

3.2. Striatal dopaminergic functioning

3.2.1. Group differences in ΔBP_{ND} during the mid task (Reward condition relative to baseline)

Striatal clusters in the left putamen, right putamen and pallidum, left caudate, and left nucleus accumbens (NAc), extending into the left

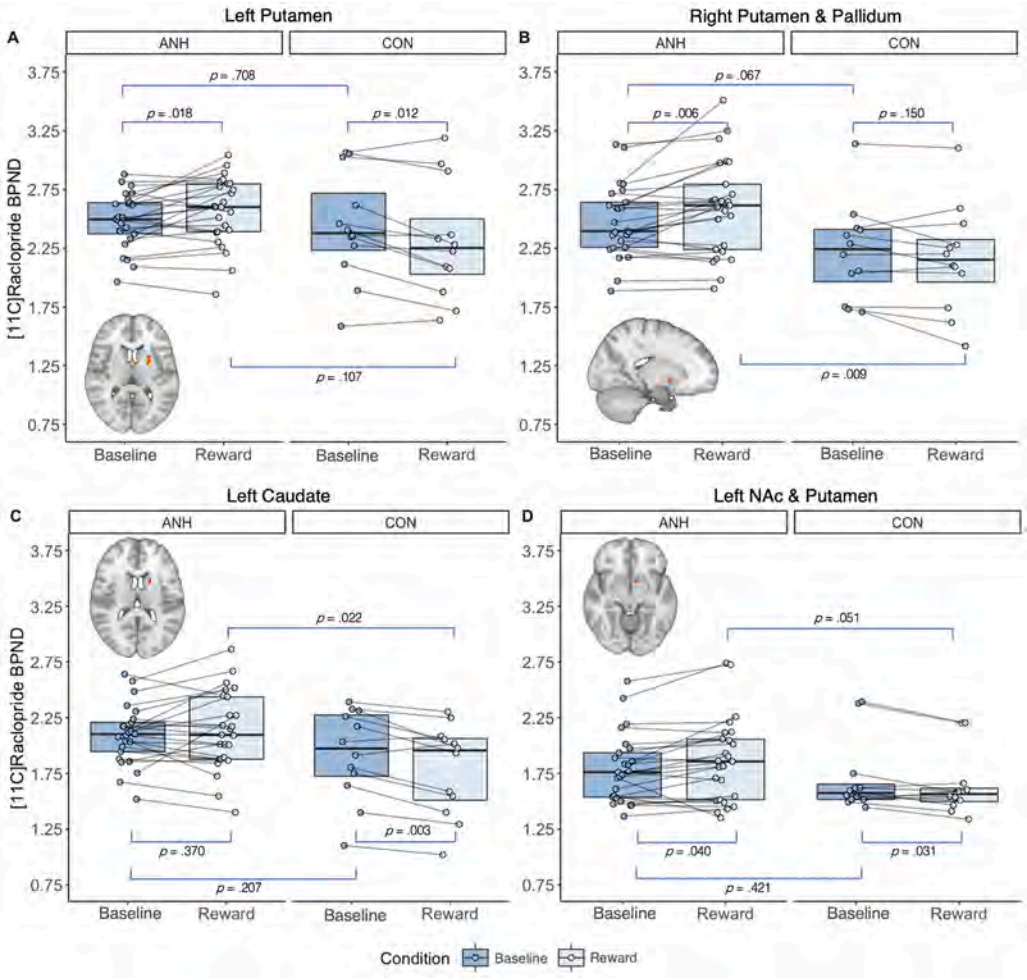

Fig. 3. [^{11}C]Raclopride binding potential in functionally-defined striatal clusters demonstrating group differences for the contrast of (ANH - CON; Reward - Baseline).
T-tests shown here (blue lines) are within-group comparisons of ΔBP_{ND} values (Reward - Baseline) and between-group comparisons of BP_{ND} values (Baseline). In each of these four clusters, there was a significant group × condition interaction, $Fs(1,20) > 7.38$, $ps < 0.010$. This was expected given that ANOVA results are dependent on the cluster-defining contrast. The baseline phase depicted here encompasses the first 42 min of scanning, from start of acquisition to start of the reward phase, including both the uptake phase and the neutral task block. (For interpretation of the references to colour in this figure legend, the reader is referred to the web version of this article.)

putamen, demonstrated between-group differences in ΔBP_{ND} values (ANH - CON) for the Reward - Baseline contrast, $F's(1,20) > 7.38$, $p's < 0.01$. These analyses controlled for sex and [^{11}C]raclopride dose, given that there were significantly fewer females in the CON group and [^{11}C]raclopride dose was, on average, higher in the ANH group. See *Table 3* for striatal cluster statistics. *Fig. 3* shows [^{11}C]raclopride BP_{ND} values for each participant by condition and group. Relative to CON participants, ANH participants showed higher [^{11}C]raclopride BP_{ND} during the reward condition relative to baseline (*Fig. 3*). This finding indicates that, relative to CON participants, ANH participants exhibited reduced task-related DA release to rewards in the striatum. Results for exploratory PET analyses are reported in Supplemental Materials IIB-IIE.

3.3. fMRI activation

Results of fMRI activation analyses are presented in Supplemental Materials IIF. ROI analyses showed a single between-group difference in right caudate activation, at an uncorrected threshold, which was not associated with clinical measures of anhedonia or self-reported stress.

3.4. fMRI connectivity

3.4.1. PET-derived seed-based general functional connectivity

Whole-brain GFC analysis revealed several significant group differences. PET-derived seeds demonstrated negative connectivity with subcortical and cortical regions in the ANH group, relative to the CON group. Target regions of these seeds included structures commonly implicated in reward processing, including bilateral caudate nucleus, putamen, and pallidum, as well as the medial prefrontal cortex. Associated regions in the anterior cingulate cortex and the thalamus were also identified as target regions. See *Table 4* for connectivity statistics. *Fig. 4* illustrates group differences in GFC between the PET-derived seeds and their respective target regions.

3.4.2. Relations between anhedonia and mesocorticolimbic network functioning

3.4.2.1. Anhedonia and task-related da release in functionally-defined striatal clusters (PET). In the ANH group, we examined associations between ΔBP_{ND} values in the above striatal clusters that demonstrated group differences and anhedonia severity scores on the SHAPS and BDI-II anhedonia subscale. Reduced task-related DA release to rewards in the left putamen cluster was significantly associated with BDI-II anhedonia scores ($\beta_{STD} = 0.47$, $SE = 0.18$, $t = 2.57$, $p = .017$, $p_{FDR} = 0.137$) (*Fig. 5*). BDI-II anhedonia subscale scores were not significantly associated with task-related DA release in the other three striatal clusters ($p's > 0.05$). SHAPS scores were not significantly associated with task-related DA release in any of the four striatal clusters ($p's > 0.05$). Results for exploratory analyses with anhedonia severity are reported in the Supplemental Materials IIG-IIH.

3.4.2.2. Anhedonia and mesocorticolimbic network connectivity (PET-MR). Neither the SHAPS nor BDI-II anhedonia subscale were significantly associated with PET-derived GFC strength for any region pairs ($p's > 0.05$) (see *Fig. 6*).

Table 4
Statistics for clusters demonstrating ANH - CON group difference in GFC seed-to-voxel analysis with PET-derived seeds. Effect sizes indicate average differences in connectivity between the two groups (ANH – CON) when controlling for age and sex. Size p-values indicate the significance of the size of the target cluster (voxels). Peak p-values indicate the significance of the signal of the target cluster, at its peak, or strongest point of connectivity. FWE, family-wise error. FDR, false-discovery rate. Unc, uncorrected. FWE and FDR are two common methods for correction of multiple comparisons. Unc p-values have not been corrected for multiple comparisons. ANH, Anhedonia participants. CON, Control participants.

Seed *Target Label* *(MNI Coordinates)*	Cluster Size (voxels)	Effect size (*b*)	Size *p*-FWE	Peak *p*-FWE	Peak *p*-unc
Left Putamen					
Bilateral Striatum (−22, 0, 6)	786	−0.21	.000	.001	.000
Right Striatum (18, 6, 8)	603	−0.13	.000	.009	.000
Right Superior Frontal Gyrus (22, −4, 62)	87	−0.08	.010	.997	.000
Right Putamen / Pallidum					
Right Striatum (18, 8, −8)	268	−0.25	.000	.003	.000
Right Paracingulate Gyrus / Anterior Cingulate Gyrus (2, 36, 26)	78	−0.08	.014	.159	.000
Right Caudate (12, 6, 12)	54	−0.09	.085	.975	.000
Left Caudate					
Bilateral Striatum / Left Thalamus (18, 18, −4)	515	−0.11	.000	.397	.000
Left Caudate (−16, 10, 20)	324	−0.27	.000	.001	.000
Left Striatum (−24, 2, −12)	99	−0.11	.005	.987	.000
Left Caudate / Thalamus (−10, −12, 16)	69	−0.09	.035	.148	.000
Left Nucleus Accumbens and Putamen					
Left Striatum (−14 6, −12)	268	−0.26	.000	.003	.000
Medial Frontal Cortex (−8, 50, −16)	57	−0.07	.065	.978	.000

3.5. Relations between self-reported stress and mesocorticolimbic network functioning

3.5.1. Self-Reported stress and task-related da release to rewards in functionally-defined striatal ROIs (PET)

Within the ANH group, analyses with the PSS and PCL-5 yielded no significant associations between self-reported stress and mesocorticolimbic task-related DA release to rewards in striatal clusters. Results for exploratory analyses with self-reported stress are reported in Supplemental Materials III-IIJ.

3.5.2. Self-Reported stress and mesocorticolimbic network connectivity (PET-MR)

Exploratory analyses with the PCL-5 yielded one significant association with GFC between the PET-derived right putamen and pallidum cluster and a target region in the paracingulate and anterior cingulate cortex; however, this association between PCL-5 scores and GFC was not significant after FDR-correction for multiple comparisons. Scores on the PSS were not significantly associated with mesocorticolimbic network connectivity.

3.6. Correlations between [^{11}C]Raclopride binding potential, fMRI network connectivity, and clinical measures

Fig. 6 summarizes bivariate Pearson correlations in the ANH group between primary and secondary clinical measures of stress and anhedonia, [^{11}C]raclopride binding potential in striatal clusters demonstrating group differences, and general functional connectivity of these striatal clusters with their respective whole-brain target regions. As hypothesized, greater [^{11}C]raclopride binding potential (i.e., reduced striatal DA release to rewards) in striatal clusters tended to be negatively associated with general functional connectivity values of these seeds and their target regions (see *Fig. 6, orange boxes in lower triangle*). However, not all of these correlations remained after an FDR-correction for multiple comparisons (see *Fig. 6, upper right triangle*).

4. Discussion

This investigation explored associations among anhedonia, striatal DA, and reward circuitry functioning in a transdiagnostic sample with clinically impairing anhedonia. Stress was also examined in an exploratory manner.

4.1. Striatal dopamine and anhedonia

Extending previous findings of decreased striatal DA release to rewards in MDD (Peciña et al., 2017; Hamilton et al., 2018), we found reduced striatal DA release to rewards in ANH participants. Interestingly, in the ANH participant group alone, there were no regions that showed a significant change in ΔBP_{ND} from baseline to the reward condition of the MID, suggesting that participants with anhedonia demonstrated blunted DA response to rewards. Next, we found that relative to the CON group, ANH participants exhibited increased [^{11}C]raclopride ΔBP_{ND} in the left and right dorsal striatum and left ventral striatum (*Fig. 3*). Together, these findings represent the first report of reduced task-related DA release to rewards in a transdiagnostic sample with clinically impairing anhedonia.

Reduced striatal DA release to rewards in ANH participants may reflect impaired reward learning (Borsini et al., 2020) although this was not seen behaviorally. The optimized MID task used here required learning which cues predicted differing reward magnitudes, enhancing the sensitivity of the task to positive prediction errors encoded by task-related DA release (Berridge and Robinson, 2003). Though we did not evaluate prediction errors *per se*, impaired modulation of behavior by rewards during a probabilistic reward task is characteristic of anhedonia in individuals with MDD (Vrieze et al., 2013; Pechtel et al., 2013). Although Hamilton and colleagues (2018) also reported lower availability of DA during baseline in an MDD sample, our findings are not consistent with this interpretation in the ANH group (Hamilton et al., 2018). That is, we did not find evidence that ANH participants were characterized by significantly lower baseline DA relative to CON participants (see *Fig. 3, for comparisons of baseline BP_{ND}*). Supplemental results for baseline differences in raclopride binding potential during baseline, using an ROI approach, are presented in Supplemental Materials IIE.

Regarding associations between striatal ΔBP_{ND} and anhedonia, we found that increased ΔBP_{ND} in the left putamen, indicative of decreased task-related DA release, was positively associated with anhedonia severity on the BDI-II anhedonia subscale. Within functionally-defined striatal clusters, SHAPS scores were not significantly related to task-related DA reward signaling, which is consistent with at least one [^{11}C]raclopride PET study in MDD (Peciña et al., 2017). These contrasting results between the BDI-II anhedonia subscale and the SHAPS may be due to differences in the aspects of anhedonia that these two scales capture. Whereas the SHAPS primarily assesses aspects of consummatory reward capacity (i.e., pleasure) (Rizvi et al., 2016; Snaith et al., 1995), the BDI-II anhedonia subscale captures aspects of both consummatory and anticipatory (i.e., motivation or interest) reward capacity (Pizzagalli et al., 2005; Snaith et al., 1995; Joiner et al., 2003). Nevertheless, our finding of an association between striatal ΔBP_{ND} and anhedonia on the BDI-II anhedonia subscale requires replication, particularly because the internal consistency of the BDI-II

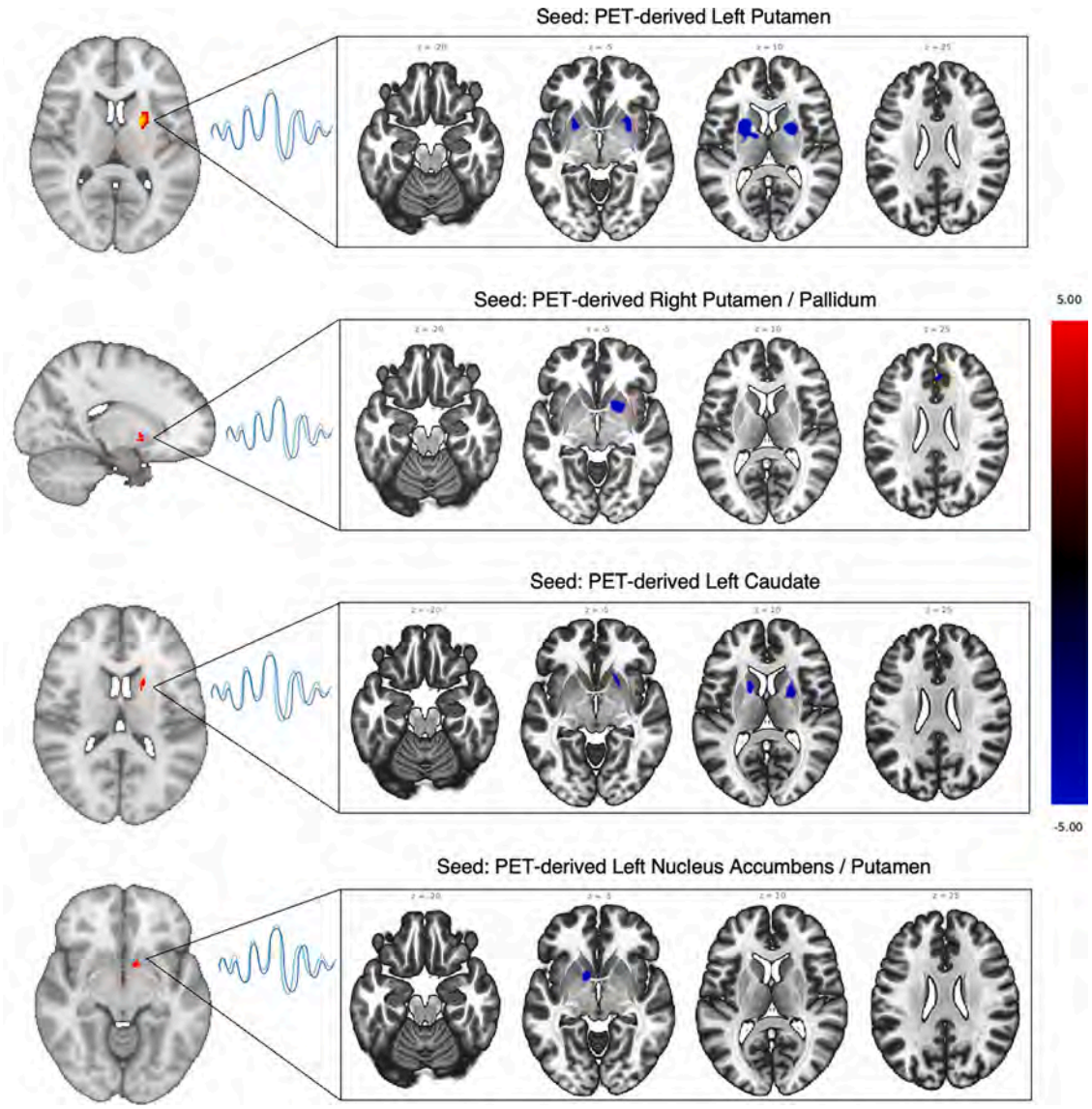

Fig. 4. Group differences in general functional connectivity of PET-derived seeds.
Seed-to-voxel analysis (ANH - CON) controlling for age and sex. Only negative connectivity values were found in the ANH group, represented in blue. PET striatal seeds are presented in radiologic view, so the left and right are reversed. ANH, Anhedonia participants. CON, Control participants. (For interpretation of the references to colour in this figure legend, the reader is referred to the web version of this article.)

anhedonia subscale is not outstanding (α = 0.60). The internal consistency of the SHAPS has been shown to be higher than the BDI-II anhedonia subscale (Nakonezny et al., 2010).

4.2. *fMRI activation during reward anticipation and reward outcome*

We did not find evidence of altered mesocorticolimbic activation during reward anticipation or reward outcome phases in ANH participants after correcting for multiple comparisons (see *Supplemental Materials IIF*). The lack of fMRI activation differences may be attributable, in part, to inadequate power of the current study to detect smaller effects given the small sample. Prior fMRI research has shown hyporesponsivity of striatal regions during anticipatory (Borsini et al., 2020; Luijten et al., 2017; Leroy et al., 2020) and consummatory processing (Nawijn et al., 2015; Ng et al., 2019; Zhang et al., 2016) in psychiatric populations where anhedonia is a central feature. As stated above, the optimized MID task used here requires learning whereas the standard fMRI MID task does not, and this could contribute to differences relative to prior MID studies. Given that DA is important for learning, the current design is an improvement with reference to DA. The current study's uncorrected fMRI activation results should be cautiously considered within the broader literature. Additionally, recent PET-MR investigations of striatal DA in MDD did not report group differences in fMRI activation during reward anticipation or reward outcomes (Hamilton et al., 2018; Schneier et al., 2018).

4.3. *Anhedonia and mesocorticolimbic general functional connectivity*

The present study also investigated functional connectivity seeded by regions exhibiting blunted striatal DA release to rewards (i.e., PET-derived seeds) using a whole-brain GFC approach. Compared to CON participants, ANH participants showed negative GFC between PET-derived seeds and several regions implicated in reward processing (i.e., bilateral caudate, putamen, and pallidum), as well as cognitive control (e.g., anterior cingulate gyrus) and control of attention (e.g., thalamus). These results are consistent with reports of altered functional cortico-striatal connectivity in MDD (Gabbay et al., 2013; Walsh et al., 2017; Kang et al., 2018) and a previous [^{11}C]raclopride PET-MR study of functional connectivity in MDD (Hamilton et al., 2018). In MDD, increased ΔBP_{ND} in the ventral striatum predicted decreased functional

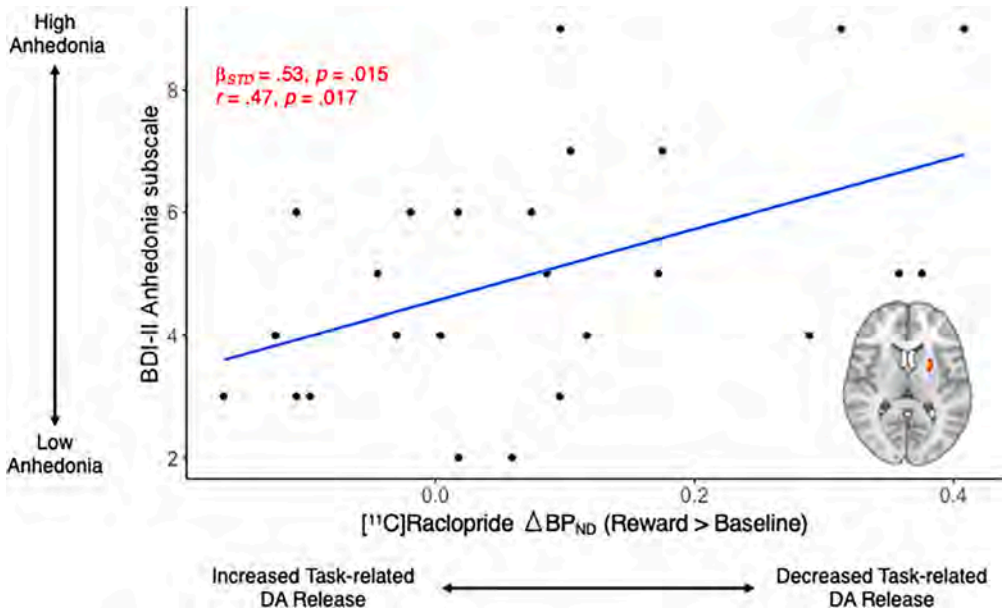

Fig. 5. Task-related DA release to rewards in the functionally-defined left putamen striatal cluster predicts BDI-II anhedonia subscale scores for ANH participants (n = 25). In ANH participants, greater [^{11}C]raclopride DBP_{ND} was associated with greater anhedonia severity on the BDI-II anhedonia subscale. Positive DBP_{ND} values represent decreased task-related DA release to rewards, relative to baseline. BDI-II, Beck Depression Inventory.

connectivity between PET-derived seeds and default-mode and salience network regions (Hamilton et al., 2018).

4.4. Impact of stress on anhedonia via striatal dopamine

Stress is believed to desensitize the mesocorticolimbic DA system and contribute to the emergence and maintenance of anhedonic behavior (Pizzagalli, 2014; Hollon et al., 2015; Valenti et al., 2012). We hypothesized that self-reported stress on the PSS would predict anhedonia severity and be associated with striatal DA release to rewards, illustrating one potential mechanism linking self-reported stress and anhedonia. This was an exploratory hypothesis, given that the current sample was not selected for their exposure to stress. Consistent with previous work (Pizzagalli, 2014; Slavich and Irwin, 2014), perceived stress and scores on the BDI-II anhedonia subscale were significantly correlated (r = 0.47). However, we did not find evidence for the contribution of self-reported stress on mesocorticolimbic DA system functioning. The PSS, our primary measure of self-reported stress, is a retrospective measure that assesses the extent to which stress is unpredictable and uncontrollable during the last month, but it does not assess different types and chronicity of stressors (Slavich and Shields, 2018). It is possible that other scales that objectively assess stressful life conditions and situations may be better suited to illuminate the role of self-reported stress in DA function. Furthermore, the nucleus accumbens (NAc) is strongly implicated in stress regulation (Stanton et al., 2018) and demonstrates a blunted response during reward consumption in patients with MDD (Pizzagalli et al., 2009). Here, group differences in dopaminergic response to rewards (*Fig. 3*) highlighted one small cluster (size=19 voxels) located between the left NAc and left putamen. We may not have found evidence of a relation between self-reported stress and mesocorticolimbic DA system functioning because these clusters were primarily located outside of the NAc.

4.5. Limitations and future directions

This study has a number of limitations. First, the sample size, though comparable to many PET studies (Baumgartner et al., 2018), was modest. As such, PET analyses are not corrected for multiple comparisons. Future work that attempts to replicate this study in larger samples should aim to use a more stringent method of statistical correction. Second, given that this is a cross-sectional study, we cannot determine causal relationships between reduced reward-related striatal DA release and anhedonia. Future research should investigate temporal relations between reduced reward-related striatal DA release and anhedonia. Third, striatal DA release may have reflected multiple reward processing components (e.g., novelty processing, associative learning). Future studies may implement alternative tasks to disentangle DA release that is solely related to rewards vs. other components activated by the MID task used here. Fourth, the current analyses estimated BP_{ND} using a two-phase model, incorporating elements of both the neutral phase and uptake phase in the baseline. Future studies may consider the tradeoff between bias and variance in deciding how to estimate BP_{ND} (Levine et al., 2022). Fifth, the ANH sample was not recruited based on severity of self-reported stress. Although the ANH sample demonstrated moderate levels of stress (see *Table 2*), the mean level of PSS scores was lower than typically reported in psychiatric samples and the variability of PSS scores was limited (Hewitt et al., 1992). Relatedly, the current study sought to examine how stress, broadly measured, relates to striatal reward responses. While we did not find any effects with respect to self-reported stress, exploring DA reward signaling during a PET-MR stress-related paradigm would be an area for future study. Sixth, while the current study did not find any dependence on total injected dose, it is possible that other unknown factors could differentially impact the dynamic uptake in the striatum and the reference region. Lastly, the length of the study presents a potential limitation on the precision of BP_{ND} estimates. Given the approximately 20-minute half-life for [11C] Raclopride, the later time frames of the dynamic PET data have poorer signal-to-noise ratios. Because the reward task is applied late in the study protocol, the BP_{ND} estimates for the reward phase are particularly sensitive to noise, particularly in the voxel-wise analysis. Future studies involving two scan visits could help to address this issue.

In summary, the present study is the first to investigate task-related striatal DA release to rewards in a transdiagnostic anhedonic sample. This study provides support for the association between blunted striatal DA functioning and transdiagnostic anhedonia. We found blunted general functional connectivity with PET-derived striatal seeds in anhedonia participants, but these group differences were not associated with anhedonia severity. We demonstrated that self-reported stress was strongly associated with anhedonia but was not associated with striatal DA. These findings provide support for the association between stress

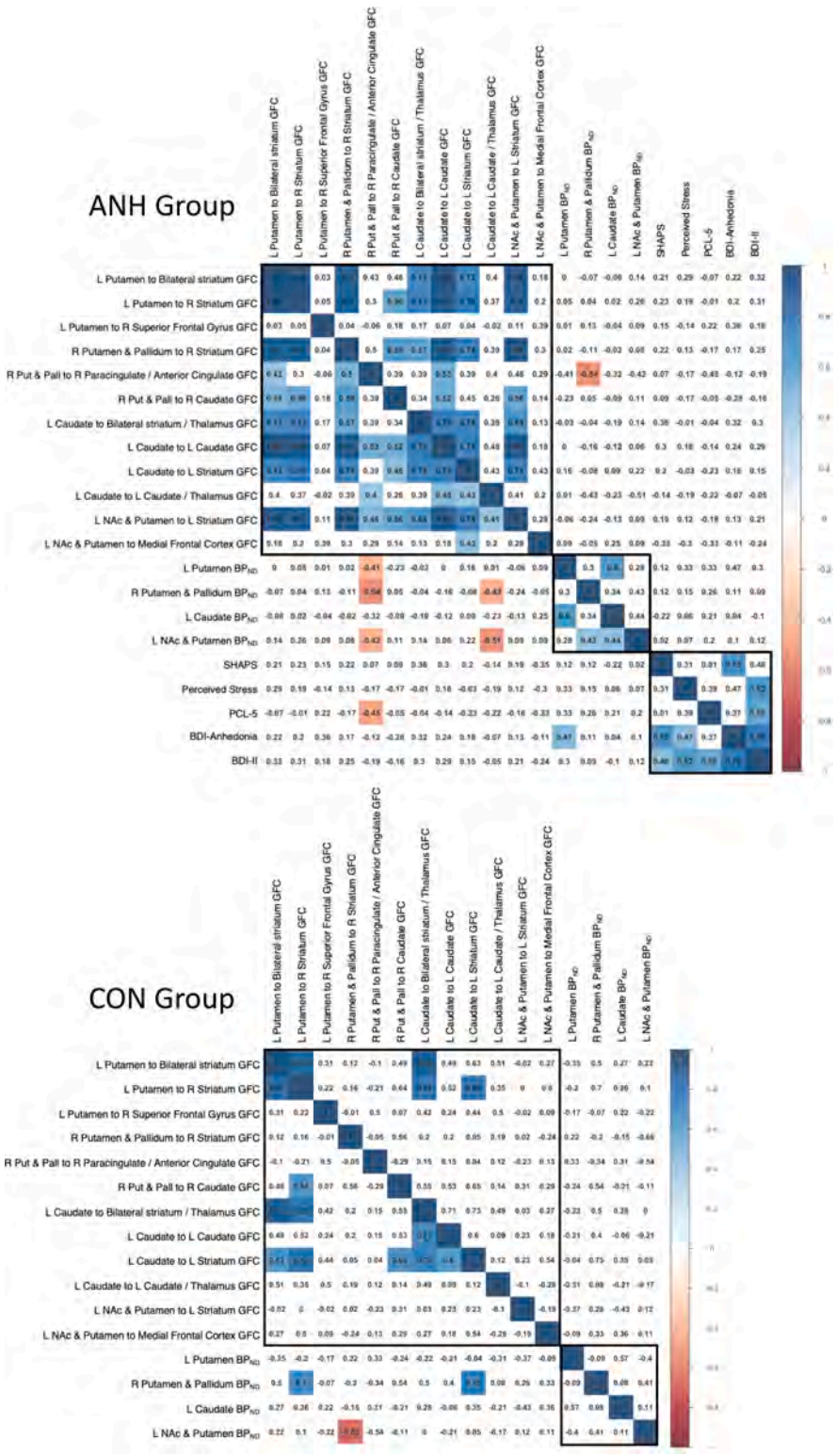

Fig. 6. Pearson correlation matrix for variables of interest.

Pearson correlation values range from −1 to 1. Significant correlations ($p < .05$) are displayed in color; non-significant correlations ($p > .05$) are displayed in white. Correlations presented in the upper right triangles of the matrices are corrected for multiple comparisons, using the false-discovery rate (FDR) method. Correlations in the lower left triangles are uncorrected. L, left. R, right. GFC, general functional connectivity. Put, Putamen. Pall, Pallidum. NAc, Nucleus Accumbens. ΔBP_{ND}, binding potential non-displacement. SHAPS, Snaith-Hamilton Pleasure Scale. PCL-5, PTSD Checklist for DSM-5. BDI, Beck Depression Inventory. ANH, Anhedonia. CON, Control.

and anhedonia and highlight a potential molecular mechanism of impaired reward processing in anhedonia-related psychopathologies.

Declaration of Competing Interest

Over the past 3 years, Dr. Pizzagalli has received consulting fees from Albright Stonebridge Group, Boehringer Ingelheim, Compass Pathways, Engrail Therapeutics, Neumora Therapeutics (formerly BlackThorn Therapeutics), Neurocrine Biosciences, Neuroscience Software, Otsuka, Sunovion, and Takeda; he has received honoraria from the Psychonomic Society (for editorial work) and from Alkermes; he has received research funding from the Brain and Behavior Research Foundation, the Dana Foundation, Millennium Pharmaceuticals, and NIMH; he has received stock options from Compass Pathways, Engrail Therapeutics, Neumora Therapeutics, and Neuroscience Software. No funding from these entities was used to support the current work, and all views expressed are

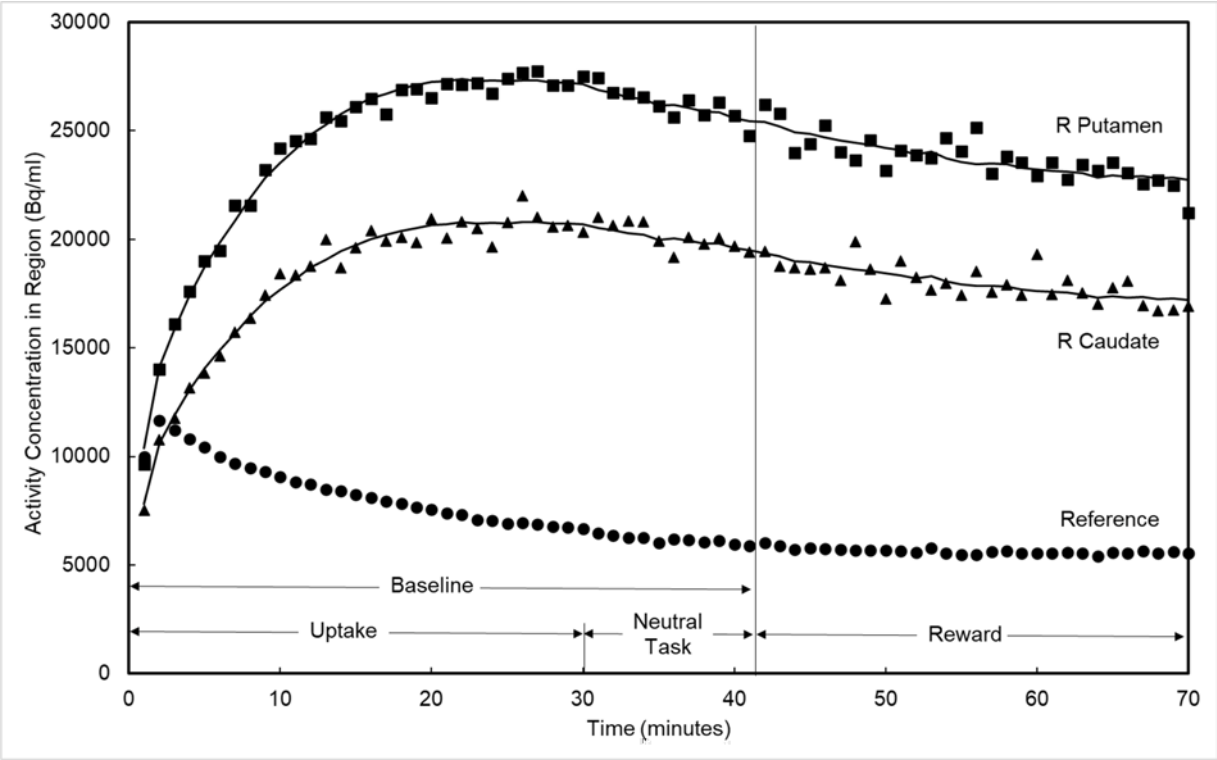

Fig. A1. Example time-activity curves (TACs) and model fits for atlas regions in one ANH subject. Raw TAC data derived from the dynamic PET images are shown as individual points and model fits are shown as solid lines. The two phases of the kinetic model, baseline and reward, are indicated along with the periods for uptake and neutral task.

solely those of the authors. The other authors have no conflicts of interest or relevant disclosures.

Acknowledgments

This research was supported by R61/R33 MH110027 to GSD and MJS, R21 MH110933 to GSD and JMH, K23 MH113733 to ECW, and UL 1TR002489. DAP was partially supported by R37 MH068376 and R01 MH095809. DD was partially supported by R01 MH111676. The content is solely the responsibility of the author and does not necessarily represent the official views of NIH.

Supplementary materials

Supplementary material associated with this article can be found, in the online version, at doi:10.1016/j.pscychresns.2023.111660.

Appendix A: Two-phase Kinetic Model

In the examination of changes to [^{11}C] BP_{ND}) for the baseline and reward-task phases. After processing the dynamic PET images and applying the registered AAL3 atlas, time-activity curves (TACs) were extracted for atlas regions (BP_{ND} maps. The baseline phase was defined from start of the bolus injection up to the start of the reward task; therefore, the baseline phase includes effects of the uptake period and the neutral-task period (Fig. A1). The reward phase was defined from start of the reward task to end of acquisition.

The SRTM model was applied with a two-phase BP_{ND} component to account for the baseline (from injection time to start of reward task) and reward states:

$$h_{baseline}(t) = exp\left(\frac{-k_2 t}{1 + BP_{ND,\ baseline}}\right) \tag{A.1}$$

$$h_{reward}(t) = exp\left(\frac{-k_2 t}{1 + BP_{ND,\ reward}}\right) \tag{A.2}$$

$$Q(t) = \sum_{t'=0}^{t_{reward}-1} TAC_{ref}(t')\ h_{baseline}(t-t') + \sum_{t'=t_{reward}}^{end} TAC_{ref}(t')\ h_{reward}(t-t') \tag{A.3}$$

$$TAC_{region}\left(t;\ R_1,\ k_2, BP_{ND,\ baseline},\ BP_{ND,\ reward}\right) =$$
$$= R_1 TAC_{ref}(t) + \left(k_2 - \frac{R_1\ k_2}{1 + BP_{ND,\ baseline}}\right) Q(t)\ if\ 0 < t < t_{reward} \quad (A.4)$$
$$= R_1 TAC_{ref}(t) + \left(k_2 - \frac{R_1\ k_2}{1 + BP_{ND,reward}}\right) Q(t)\ if\ t \geq t_{reward}$$

Where

- $t = 0$ represents the start of the scan at time of bolus injection
- $h_{baseline}(t)$ and $h_{reward}(t)$ are the exponential system impulse responses in the reward and neutral states, respectively;
- $Q(t)$ is a time-dependent discrete convolution of the reference time-activity curve (TAC) with the system response kernels accounting for the reward and neutral conditions;
- $TAC_{region}(t)$ represents the TAC of a given atlas region or voxel;
- $TAC_{ref}(t)$ represents the TAC for the cerebellar reference region (measured from the cerebellar regions of the AAL3 atlas, excluding regions labeled as vermis);
- R_1 is an estimated parameter of the SRTM model representing the ratio of kinetic transport rates from plasma to free-tracer tissue compartments in the TAC region studied and reference region;
- k_2 is an estimated parameter of the SRTM model representing the kinetic transport rate from free-tracer tissue to plasma compartments in the TAC region studied;
- $BP_{ND,\ baseline}$ and $BP_{ND,\ reward}$ are estimated parameters representing the non-displaceable binding potential in each of the two phases, Baseline and Reward, respectively;
- t_{reward} is the time at which the reward task is begun (usually 42 min into the study but varied for individual subjects based on the recorded task start time; the baseline binding potential is estimated from injection up to start of reward block).

For each TAC, the two-phase model was fitted with a custom MATLAB script applying a nonlinear least-squares fit to the model equations. Thus, for each subject and for each hypothesized atlas region or voxel, we obtained estimates of $BP_{ND,\ baseline}$ and $BP_{ND,\ reward}$as well as phase-independent parameters R_1 and k_2 . A composite region of cerebellum-labeled regions from the AAL3 atlas was used to compute the reference TAC.

References

Anderson, J.S., Ferguson, M.A., Lopez-Larson, M., Yurgelun-Todd, D., 2011. Reproducibility of Single-Subject Functional Connectivity Measurements. Am. J. Neuroradiol 32, 548–555.

Antoniuk, S., Bijata, M., Ponimaskin, E., Wlodarczyk, J., 2019. Chronic unpredictable mild stress for modeling depression in rodents: meta-analysis of model reliability. Neurosci. Biobehav. Rev 99, 101–116.

Arrondo, G., Segarra, N., Metastasio, A., Ziauddeen, H., Spencer, J., Reinders, N.R., et al., 2015. Reduction in ventral striatal activity when anticipating a reward in depression and schizophrenia: a replicated cross-diagnostic finding. Front. Psychol 6, 1280.

Baumgartner, R., Joshi, A., Feng, D., Zanderigo, F., Ogden, R.T., 2018. Statistical evaluation of test-retest studies in PET brain imaging. Ejnmmi. Res 8 (13).

Benjamani, Y., Hochberg, Y., 1995. A Practical and Powerful Approach to Multiple Testing: a Practical and Powerful Approach to Multiple Testing. J. Royal. Statist. Society 57, 289–300.

Bernstein, D.P., Fink, L., Handelsman, L., Foote, J., Lovejoy, M., Wenzel, K., et al., 1994. Initial reliability and validity of a new retrospective measure of child abuse and neglect. Am. J. Psychiat 151, 1132–1136.

Berridge, K.C., Kringelbach, M.L., 2008. Affective neuroscience of pleasure: reward in humans and animals. Psychopharmacology. (Berl.) 199, 457–480.

Berridge, K.C., Robinson, T.E., 2003. Parsing reward. Trends. Neurosci. 26, 507–513.

Blevins, C.A., Weathers, F.W., Davis, M.T., Witte, T.K., Domino, J.L., 2015. The posttraumatic stress disorder checklist for DSM-5 (PCL-5): development and Initial Psychometric Evaluation. J. Trauma. Stress 28, 489–498.

Borsini, A., Wallis, A.S.J., Zunszain, P., Pariante, C.M., Kempton, M.J., 2020. Characterizing anhedonia: a systematic review of neuroimaging across the subtypes of reward processing deficits in depression. Cogn.. Affect. Behav.. Neurosci. 1–26.

Cabib, S., Puglisi-Allegra, S., 2012. The mesoaccumbens dopamine in coping with stress. Neurosci. Biobehav. Rev 36, 79–89.

Cohen, S., Janicki-Deverts, D., 2012. Who\'s Stressed? Distributions of Psychological Stress in the United States in Probability Samples from 1983, 2006, and 20091. J. Appl. Soc. Psychol 42, 1320–1334.

Cohen, S., Kamarck, T., Mermelstein, R., 1983. A Global Measure of Perceived Stress. J. Health. Soc. Behav 24, 385.

Der-Avakian, A., Markou, A., 2012. The neurobiology of anhedonia and other reward-related deficits. Trends. Neurosci 35, 68–77.

Elliott, M.L., Knodt, A.R., Cooke, M., Kim, M.J., Melzer, T.R., Keenan, R., et al., 2019. General functional connectivity: shared features of resting-state and task fMRI drive reliable and heritable individual differences in functional brain networks. Neuroimage 189, 516–532.

Felger, J.C., Li, Z., Haroon, E., Woolwine, B.J., Jung, M.Y., Hu, X., Miller, A.H., 2015. Inflammation is associated with decreased functional connectivity within corticostriatal reward circuitry in depression. Mol. Psychiatr 21, 1358–1365.

First, M., Karg, R., Williams, J., Spitzer, R., 2015. Structured Clinical Interview For DSM-5-Research Version (SCID-5 For DSM-5, Research Version; SCID-5-RV). American Psychiatric Association.

Franken, I.H.A., Rassin, E., Muris, P., 2007. The assessment of anhedonia in clinical and non-clinical populations: further validation of the Snaith–Hamilton Pleasure Scale (SHAPS). J. Affect. Disorders 99, 83–89.

Gabbay, V., Ely, B.A., Li, Q., Bangaru, S.D., Panzer, A.M., Alonso, C.M., et al., 2013. Striatum-based circuitry of adolescent depression and anhedonia. J. Am. Acad. Child. Adolesc. Psychiatry 52, 628–641 e13.

Gasperi, M., Afari, N., Goldberg, J., Suri, P., Panizzon, M.S., 2021. Pain and Trauma: the role of criterion a trauma and stressful life events in the pain and PTSD relationship. J. Pain 22, 1506–1517.

Hamilton, J.P., Sacchet, M.D., Hjørnevik, T., Chin, F.T., Shen, B., Kämpe, R., et al., 2018. Striatal dopamine deficits predict reductions in striatal functional connectivity in major depression: a concurrent 11C-raclopride positron emission tomography and functional magnetic resonance imaging investigation. Transl. Psychiat 8, 264.

Hanson, J.L., Williams, A.V., Bangasser, D.A., Peña, C.J., 2021. Impact of Early Life Stress on Reward Circuit Function and Regulation. Front. Psych. 12, 744690.

Hewitt, P.L., Flett, G.L., Mosher, S.W., 1992. The Perceived Stress Scale: factor structure and relation to depression symptoms in a psychiatric sample. J. Psychopathol. Behav 14, 247–257.

Hollon, N.G., Burgeno, L.M., Phillips, P.E.M., 2015. Stress effects on the neural substrates of motivated behavior. Nat. Neurosci 18, 1405–1412.

Husain, M., Roiser, J.P., 2018. Neuroscience of apathy and anhedonia: a transdiagnostic approach. Nat.. Rev.. Neurosci. 19, 470–484.

Joiner, T.E., Brown, J.S., Metalsky, G.I., 2003. A test of the tripartite model\'s prediction of anhedonia\'s specificity to depression: patients with major depression versus patients with schizophrenia. Psychiat. Res 119, 243–250.

Kadouri, A., Corruble, E., Falissard, B., 2007. The improved Clinical Global Impression Scale (iCGI): development and validation in depression. BMC. Psychiatry 7, 7.

Kang, L., Zhang, A., Sun, N., Liu, P., Yang, C., Li, G., et al., 2018. Functional connectivity between the thalamus and the primary somatosensory cortex in major depressive disorder: a resting-state fMRI study. BMC. Psychiatry 18, 339.

Krishnan, V., Han, M.H., Graham, D.L., Berton, O., Renthal, W., Russo, S.J., et al., 2007. Molecular adaptations underlying susceptibility and resistance to social defeat in brain reward regions. Cell 131, 391–404.

Kumar, P., Slavich, G.M., Berghorst, L.H., Treadway, M.T., Brooks, N.H., Dutra, S.J., et al., 2015. Perceived Chronic Stress Exposure Modulates Reward-Related Medial Prefrontal Cortex Responses to Acute Stress in Depression. J. Affect. Disorders 180, 104–111.

Ladefoged, C.N., Law, I., Anazodo, U., KSt, Lawrence, Izquierdo-Garcia, D., Catana, C., et al., 2017. A multi-centre evaluation of eleven clinically feasible brain PET/MRI attenuation correction techniques using a large cohort of patients. Neuroimage 147, 346–359.

Lammertsma, A.A., Hume, S.P., 1996. Simplified Reference Tissue Model for PET Receptor Studies. Neuroimage 4, 153–158.

Leroy, A., Amad, A., D\'Hondt, F., Pins, D., Jaafari, N., Thomas, P., Jardri, R., 2020. Reward anticipation in schizophrenia: a coordinate-based meta-analysis. Schizophr. Res 218, 2–6.

Levine, M.A., Mandeville, J.B., Calabro, F., Izquierdo-Garcia, D., Chonde, D.B., Chen, K. T., et al., 2022. Assessment of motion and model bias on the detection of dopamine response to behavioral challenge. J. Cereb. Blood. Flow. Metabolism 42, 1309–1321.
Liu, R., Wang, Y., Chen, X., Zhang, Z., Xiao, L., Zhou, Y., 2021. Anhedonia correlates with functional connectivity of the nucleus accumbens subregions in patients with major depressive disorder. Neuroimage. Clin 30, 102599.
Luijten, M., Schellekens, A.F., Kühn, S., Machielse, M.W.J., Sescousse, G., 2017. Disruption of Reward Processing in Addiction : an Image-Based Meta-analysis of Functional Magnetic Resonance Imaging Studies. Jama. Psychiat 74, 387.
Nakonezny, P.A., Carmody, T.J., Morris, D.W., Kurian, B.T., Trivedi, M.H., 2010. Psychometric evaluation of the Snaith–Hamilton pleasure scale in adult outpatients with major depressive disorder. Int. Clin. Psychopharm 25, 328–333.
Nawijn, L., Zuiden, M van, Frijling, J.L., Koch, S.B.J., Veltman, D.J., Olff, M., 2015. Reward functioning in PTSD: a systematic review exploring the mechanisms underlying anhedonia. Neurosci. Biobehav. Rev 51, 189–204.
Ng, T.H., Alloy, L.B., Smith, D.V., 2019. Meta-analysis of reward processing in major depressive disorder reveals distinct abnormalities within the reward circuit. Transl. Psychiat 9, 293.
Papenberg, G., Jonasson, L., Karalija, N., Johansson, J., Köhncke, Y., Salami, A., et al., 2019. Mapping the landscape of human dopamine D2/3 receptors with [11C] raclopride. Brain. Struct. Funct 224, 2871–2882.
Pechtel, P., Dutra, S.J., Goetz, E.L., Pizzagalli, D.A., 2013. Blunted reward responsiveness in remitted depression. J. Psychiatr. Res 47, 1864–1869.
Peciña, M., Sikora, M., Avery, E.T., Heffernan, J., Peciña, S., Mickey, B.J., Zubieta, J.K., 2017. Striatal dopamine D2/3 receptor-mediated neurotransmission in major depression: implications for anhedonia, anxiety and treatment response. Eur. Neuropsychopharm 27, 977–986.
Pizzagalli, D.A., Jahn, A.L., O\'Shea, J.P., 2005. Toward an objective characterization of an anhedonic phenotype: a signal-detection approach. Biol. Psychiat 57, 319–327.
Pizzagalli, D.A., Holmes, A.J., Dillon, D.G., Goetz, E.L., Birk, J.L., Bogdan, R., et al., 2009. Reduced Caudate and Nucleus Accumbens Response to Rewards in Unmedicated Individuals With Major Depressive Disorder. Am. J. Psychiat 166, 702–710.
Pizzagalli, D.A., Berretta, S., Wooten, D., Goer, F., Pilobello, K.T., Kumar, P., et al., 2019. Assessment of striatal dopamine transporter binding in individuals with major depressive disorder. Jama. Psychiat 76, 854–861.
Pizzagalli, D.A., 2014. Depression, Stress, and Anhedonia: toward a Synthesis and Integrated Model. Clin.. Psychol. 10, 393–423.
Riga, D., Theijs, J.T., Vries, T.J.D., Smit, A.B., Spijker, S., 2015. Social defeat-induced anhedonia: effects on operant sucrose-seeking behavior. Front. Behav. Neurosci 9, 195.
Rizvi, S.J., Pizzagalli, D.A., Sproule, B.A., Kennedy, S.H., 2016. Assessing anhedonia in depression: potentials and pitfalls. Neurosci. Biobehav. Rev 65, 21–35.
Russo, S.J., Nestler, E.J., 2013. The brain reward circuitry in mood disorders. Nature. Reviews. Neuroscience 14. https://doi.org/10.1038/nrn3381.
Sander, C.Y., Hooker, J.M., Catana, C., Rosen, B.R., Mandeville, J.B., 2016. Imaging Agonist-Induced D2/D3 Receptor Desensitization and Internalization In Vivo with PET/fMRI. Neuropsychopharmacol 41, 1427–1436.
Schneier, F.R., Slifstein, M., Whitton, A.E., Pizzagalli, D.A., Reinen, J., McGrath, P.J., et al., 2018. Dopamine release in antidepressant-naive major depressive disorder: a Multimodal [11C]-(+)-PHNO positron emission tomography and functional magnetic resonance imaging Study. Biol. Psychiat 84, 563–573.
Schott, B.H., Minuzzi, L., Krebs, R.M., Elmenhorst, D., Lang, M., Winz, O.H., et al., 2008. Mesolimbic functional magnetic resonance imaging activations during reward anticipation correlate with reward-related ventral striatal dopamine release. J. Neurosci 28, 14311–14319.
Schultz, W., 2019. Recent advances in understanding the role of phasic dopamine activity. *F1000research*. 8. F1000 Faculty Rev-1680.
Siegel, J.S., Power, J.D., Dubis, J.W., Vogel, A.C., Church, J.A., Schlaggar, B.L., Petersen, S.E., 2014. Statistical improvements in functional magnetic resonance imaging analyses produced by censoring high-motion data points. Hum. Brain. Mapp 35, 1981–1996.
Slavich, G.M., Irwin, M.R., 2014. From Stress to Inflammation and Major Depressive Disorder: a Social Signal Transduction Theory of Depression. Psychol. Bull 140, 774–815.
Slavich, G.M., Shields, G.S., 2018. Assessing Lifetime Stress Exposure Using the Stress and Adversity Inventory for Adults (Adult STRAIN). Psychosom. Med 80, 17–27.
Smarr, K.L., Keefer, A.L., 2011. Measures of depression and depressive symptoms: beck Depression Inventory-II (BDI-II), Center for Epidemiologic Studies Depression Scale (CES-D), Geriatric Depression Scale (GDS), Hospital Anxiety and Depression Scale (HADS), and Patient Health Questionnaire-9 (PHQ-9). Arthrit. Care. Res 63, S454–S466.
Snaith, R.P., Hamilton, M., Morley, S., Humayan, A., Hargreaves, D., Trigwell, P., 1995. A Scale for the Assessment of Hedonic Tone the Snaith–Hamilton Pleasure Scale. Brit. J. Psychiat 167, 99–103.
Soares, J.M., Sampaio, A., Ferreira, L.M., Santos, N.C., Marques, F., Palha, J.A., et al., 2012. Stress-induced changes in human decision-making are reversible. Transl. Psychiat 2, e131 e131.
Stanton, C.H., Holmes, A.J., Chang, S.W.C., Joormann, J., 2018. From Stress to Anhedonia: molecular Processes through Functional Circuits. Trends. Neurosci 42, 23–42.
Stringaris, A., Belil, P.V.R., Artiges, E., Lemaitre, H., Gollier-Briant, F., Wolke, S., et al., 2015. The brain\'s response to reward anticipation and depression in adolescence: dimensionality, specificity, and longitudinal predictions in a community-based sample. Am. J. Psychiat 172, 1215–1223.
Team RC (2020): R: a language and environment for statistical computing. Retrieved from https://www.R-project.org/.
Valenti, O., Gill, K.M., Grace, A.A., 2012. Different stressors produce excitation or inhibition of mesolimbic dopamine neuron activity: response alteration by stress pre-exposure. Eur. J. Neurosci 35, 1312–1321.
Vrieze, E., Pizzagalli, D.A., Demyttenaere, K., Hompes, T., Sienaert, P., Boer, P de, et al., 2013. Reduced Reward Learning Predicts Outcome in Major Depressive Disorder. Biol. Psychiat 73, 639–645.
Wacker, J., Dillon, D.G., Pizzagalli, D.A., 2009. The role of the nucleus accumbens and rostral anterior cingulate cortex in anhedonia: integration of resting EEG, fMRI, and volumetric techniques. Neuroimage 46, 327–337.
Walsh, E., Carl, H., Eisenlohr-Moul, T., Minkel, J., Crowther, A., Moore, T., et al., 2017. Attenuation of frontostriatal connectivity during reward processing predicts response to psychotherapy in major depressive disorder. Neuropsychopharmacol 42, 831–843.
Whitfield-Gabrieli, S., Nieto-Castanon, A., 2012. Conn: a Functional Connectivity Toolbox for Correlated and Anticorrelated Brain Networks. Brain. Connect 2, 125–141.
Willner, P., Muscat, R., Papp, M., 1992. Chronic mild stress-induced anhedonia: a realistic animal model of depression. Neurosci. Biobehav. Rev 16, 525–534.
Zhang, B., Lin, P., Shi, H., Öngür, D., Auerbach, R.P., Wang, X., et al., 2016. Mapping anhedonia-specific dysfunction in a transdiagnostic approach: an ALE meta-analysis. Brain. Imaging. Behav 10, 920–939.
Zürcher, N.R., Walsh, E.C., Phillips, R.D., Cernasov, P.M., Tseng, C.E.J., Dharanikota, A., et al., 2021. A simultaneous [11C]raclopride positron emission tomography and functional magnetic resonance imaging investigation of striatal dopamine binding in autism. Transl. Psychiat 11, 33.